Physical Layer Performance of a Cooperative Amplify and Forward Scheme for MIMO WLANs

Yuepeng Qi, Student Member, IEEE, and Mihail L. Sichitiu, Member, IEEE

Abstract—This paper proposes a novel cooperative amplify and forward (CAF) architecture for MIMO WLANs to improve their coverage and transmission rates, without requiring any modifications in the IEEE 802.11 standards at the clients. System models are used for analyzing physical layer of CAF networks, and compared with conventional amplify-and-forward (AF) and decode-and-forward (DF) networks. Numerical results demonstrate that CAF network clearly outperforms conventional 802.11 networks, AF and DF networks in terms of coverage and throughput.

Index Terms—Cooperative Systems, diversity, fading channels, MIMO systems, relays, transceivers, wireless LAN.

I. INTRODUCTION

Over the last twenty years, we have seen an exciting success of IEEE 802.11 networks in meeting the tremendously increasing demand for bandwidth. The latest IEEE 802.11 standards, 802.11ax and 802.11ay, provide up to 9.6 Gbps and 20 Gbps data rates at ranges of about 100 and 10 meters respectively. Meanwhile, mobile carriers, facing an RF shortage, are densely building small cellular cells (ranged from 10m to 1000m) to meet customers' increasingly demanding for speed. According to Signals Research Group, mobile data traffic in the United States alone is expected to grow between 53 times and 153 times from 2010 to 2020, while cellular network capacity will grow by only approximately 25 times [1]. The IEEE 802.11 networks with extended range represent an attractive approach capable to fill that gap. Compared with cellular systems, IEEE 802.11 networks are inexpensive and accessible by more wireless devices, even those without cellular service capability, like laptops and tablets.

Since IEEE 802.11 was designed for indoor environments, the coverage of an access point (AP) is rather limited. In order to cover a wide area with a reasonably low number of APs, the AP coverage needs to be extended. The problem is that, due to cost, size and power limitation, mobile stations (MSs) typically have low transmission power and low antenna gain, which limits their transmission ranges. Hence, merely increasing the transmit power of AP does not necessarily increase the WLAN coverage, if the WLAN uplinks are not improved correspondingly.

Copyright (c) 2015 IEEE. Personal use of this material is permitted. However, permission to use this material for any other purposes must be obtained from the IEEE by sending a request to pubs-permissions@ieee.org.

Y. Qi is with the Department of Computer Science, North Carolina State University, Raleigh, NC, 27695 USA (e-mail: yqi@ncsu.edu).

M.L. Sichitiu is with the Department of Electrical and Computer Engineering, North Carolina State University, Raleigh, NC, 27695 USA (e-mail: mlsichit@ncsu.edu).

TABLE I SUMMARY OF RELATED WORK CONTRIBUTIONS $^{\mathrm{1}}$

	AF	SDM	MB	MH	MBMH	WLAN
[2]–[6]		✓				
[7]			\checkmark			
[8]–[10]	✓	\checkmark		2		
[11]	✓			2		
[12]	✓	2		2		
[13]	✓		\checkmark	\checkmark		
[14]	✓	\checkmark	\checkmark			
[15]	✓	\checkmark		\checkmark		
[16]	✓		2	2		\checkmark
[17]			\checkmark	\checkmark		
[18]	✓			\checkmark		
[19], [20]			SE	\checkmark	SE	
[21]		\checkmark	SE	2	SE	
[22]*	✓	\checkmark	2	2	2	
This work	✓	✓	✓	✓	✓	✓

We propose a novel cooperative amplify and forward (CAF) scheme for MIMO spatial division multiplexing (SDM) WLANs, aiming at extending the coverage of WLAN cells, with no modifications on the MSs or IEEE 802.11 standards. In a CAF WLAN, several low-cost amplify and forward (AF) relays are deployed around the AP, with disjoint local channels. Every AF relay listens to its local channel and forwards signals immediately to a common channel, and vice versa (i.e., forwards signals from the common channel to the local channel). For the uplink from an MS to the AP, packets are forwarded by multiple relays and combined at the AP. For the downlink of CAF, packets transmitted from the AP are forwarded by one relay and delivered directly to the target MS. Although only one copy is received by targeted MS, the downlink range is still considerably expanded if the highgain antenna and high-power are used at the AP and relays. Importantly, using these AF relays requires no changes on the existing functionality of MSs.

In order to analyze and compare the PHY performance of CAF with conventional AF and decode-and-forward (DF) schemes, we model multi-branch multi-hop MIMO (SDM) relay systems. Many of the components we used have been presented in other papers before, but, to the best of our

¹Terms MB, MH and MBMH stand for multi-branch, multi-hop and the combination of these two, respectively. By "2" we denote the maximum number of antennas/branches/hops considered in the corresponding papers. In the MB and MBMH columns, term SE means the selective path scheme is adopted. Work [22] uses OSTBC.

knowledge, not combined to model the relay network we consider in this paper. We review the papers including these components and some other papers related to ours. Table I summarizes the contributions of these related works in contrast to the work in this paper.

For the *bit error rate* (BER) analysis of a multi-branch network, the PDF of combined SNR can be calculated through *M*-fold integrals over the marginal PDF of every single-branch SNR, where *M* depends on the number of branches [4]. Computation of this, however, can be costly when the number of branches increases. M.K. Simon and M.S. Alouini proposed a moment-generating function (MGF) approach for calculating the BER of a channel in [4], [5]. In their approach, the average BER was obtained by taking only one integral of the product of all single-branch SNRs' MGFs. This approach, later, was widely utilized for analyzing the BER of networks. For instance, in [23], the BER of a single hop MIMO (beamforming) channel was analyzed following the MGF approach.

To calculate the BER of a multi-hop AF network, the distribution of end-to-end (e2e) instantaneous SNR is required. In [11], authors proposed a harmonic mean approach to calculate the PDF of SNR of a dual-hop SISO link. In their work, the PDF of e2e SNR was obtained by calculating the reciprocal of harmonic mean of two single-hop SNRs' PDFs. The harmonic mean is solvable by using MGF approach mentioned earlier, with knowledge of PDF of each single-hop SNR's reciprocal. This approach was afterwards adopted in [10] for calculating the BER of a dual-hop AF relay MIMO (beamforming) network. A recent paper [12] calculated the BER of a dual-hop AF MIMO (two-by-two, beamforming) network. It obtained the MGF of the e2e SNR by calculating each conditional MGF. However, this method is hard to extend to the general case, since integration over all conditional MGFs can be very difficult given the fact that expressions of the conditional MGFs are complicated even for a simple fading channel. In [18], a general multi-hop SISO link is considered, and a closed-form expression for average BER is derived, but without an extension to MIMO links.

All approaches mentioned above compute the exact BER of a network. They require integrals of the product of instantaneous symbol error rate (SER) with the PDF of instantaneous SNR. The calculations of these integrals can be more difficult for a network with the combination of multi-branch, multi-hop and MIMO features, since the PDF of the e2e SNR is very complicated and its closed-form may be impossible to obtain. Arising from such difficulty, an asymptotic approach for calculating BER is proposed: in [7], authors show that, in the case of high SNR, the average SER is dominated by the behavior of the normalized SNR close to zero. Therefore the PDF of instantaneous SNR can be simply expressed by a Taylor series expansion at zero. Comparing with the exact BER analysis, the asymptotic approach is much more convenient for calculating the average BER. This asymptotic approach was adopted widely by the research on PHY performance evaluations of relay networks: in [13], authors analyzed a multi-hop and multi-branch SISO network, given the exact values of PDF of each hop and each branch SNR at zero; Luis G. Ordóñez et al. in [3] obtained the asymptotic average BER of a single-hop

MIMO (SDM) network; based on [3], C. Song et al. analyzed a dual-hop AF relay MIMO (SDM) network [8] [9]; in [14], a relay system, equipped with a large group of AF MIMO relays far away from source and destination nodes, is analyzed by assuming no relay-to-relay communications, and using simple ZF equalizers. A recent research [15] calculated the average BER of a multi-hop MIMO (beamforming) network following the same asymptotic approach. However, none of the works above considers a multi-branch multi-hop MIMO (SDM) link similar to ours.

In [16], authors proposed an asynchronous AF relay scheme to enhance the PHY performance of SISO WLANs, by selecting exactly two mobile nodes as AF relays for each transmission. The authors assume modified IEEE 802.11 MAC and physical layers at the AP, mobile stations and relays. They call the new MAC layer R-MAC. In their approach, each transmission takes two consecutive time slots. For the first time slot, the source node transmits signals to the two relay nodes using an Orthogonal Space-Time Block Code (OSTBC) scheme, which is similar to the setting adopted in [22]. Upon reception of signals from the source node, these relays switch their circuits from receive to transmit mode and then forward the amplified signals to the destination node in the second time slot. Simulation results show that their proposed scheme can achieve a 50% throughput gain over the conventional IEEE 802.11 scheme. The approach proposed in [16] modifies IEEE 802.11 standards on all devices for both PHY and MAC layers, and only considers SISO mode. In contrast, our proposed CAF solution for WLAN does not require modifications at the clients, requires no change in IEEE 802.11 standards, and accommodates MIMO mode.

While related works reviewed above consider AF relay systems, others analyze DF relay systems. In DF systems, the relay attempts to decode the received frame and re-encode it before retransmitting it. Works in [17], [19]–[21] considered DF relaying and derived BERs for a multi-branch dual-hop SISO system, a multi-hop SISO system, a multi-branch multi-hop SISO system, and a dual-hop dual-branch MIMO system respectively. A relay selection scheme was proposed in [24] to maximize the coverage region of cellular networks by deploying DF relays. In comparison with an AF relay, a DF relay requires more computation resources, consumes more energy, and adds more delay.

In this work, we propose and analyze a CAF scheme for WLANs by deploying low-cost, low-complexity AF relays. The main contributions of this paper are summarized as follows:

- We propose a novel cooperative multi-channel MIMO (SDM) relay system to extend the coverage of IEEE 802.11 networks and improve their transmission rates. Importantly, our proposed scheme does not require modifications at the clients, and requires no modification in IEEE 802.11 standards.
- 2) We develop a model to analyze the BER performance of multi-branch multi-hop MIMO (SDM) networks (e.g., CAF system). Although individual components of this model has been used in modeling other systems as shown in Table I, to the best of our knowledge, none of

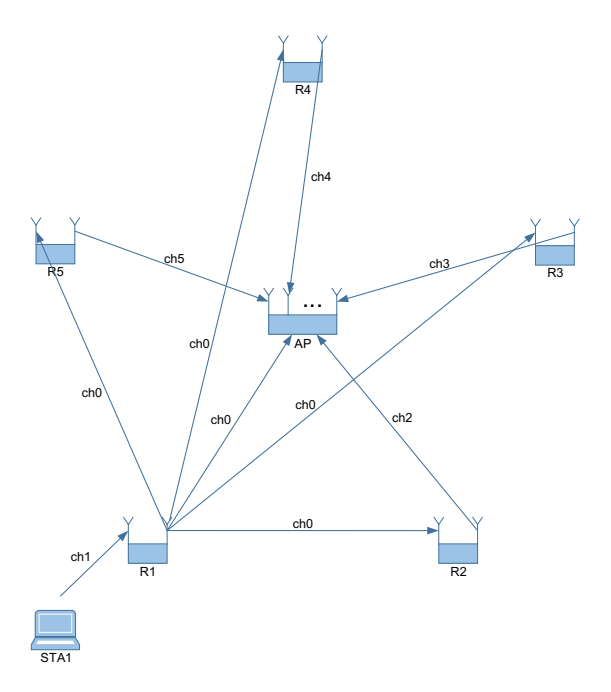


Fig. 1. Relay strategies of CAF uplink, deployed with one AP and 5 relays.

the previous papers have considered and theoretically analyzed a system similar to the one proposed in this paper, and our model fills that gap. To reduce the complexity of the model, we propose a MGF-based approach, which simplifies the BER calculation of CAF system to a single integration over a close-form expression.

3) We provide analytical and simulation results to show the performance of the proposed CAF scheme, in comparison with conventional AF and DF schemes. Specifically, BER, transmission rates, and coverage are studied and compared for CAF, AF and DF schemes for both uplink and downlink cases.

The rest of this paper is organized as follows: Sections II and III describe the CAF, conventional AF, and DF networks, and present system models of these networks. Section IV analyzes BERs of these networks and furthermore estimates and compares their coverage. In Section V we evaluate their performance from both theoretical and simulation results. At last, Section VI concludes this paper and presents our future work.

II. RELAY STRATEGIES

A. Cooperative Multi-channel Amplify and Forward Relay Strategy

For a CAF network with L relays, we need L+1 orthogonal channels: one *common channel* and L *local channels*. Every relay is equipped with two sets of antenna arrays, one of which is set to a common channel (we will call this channel 0 in Fig. 1) and the other is set to a local channel. The relays follow two straightforward rules:

 When a relay detects one channel busy and the other idle, it amplifies and forwards the signal from the busy channel to the idle channel immediately.

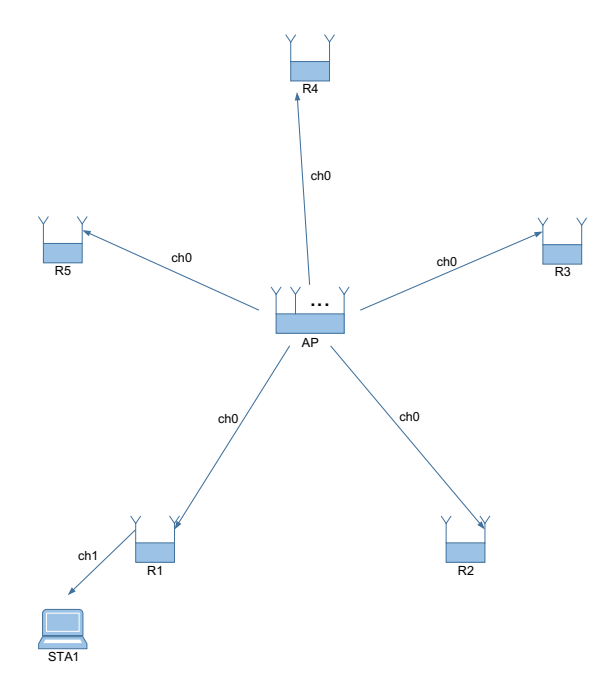


Fig. 2. Relay strategies of CAF/AF/DF downlink, deployed with one AP and 5 relays.

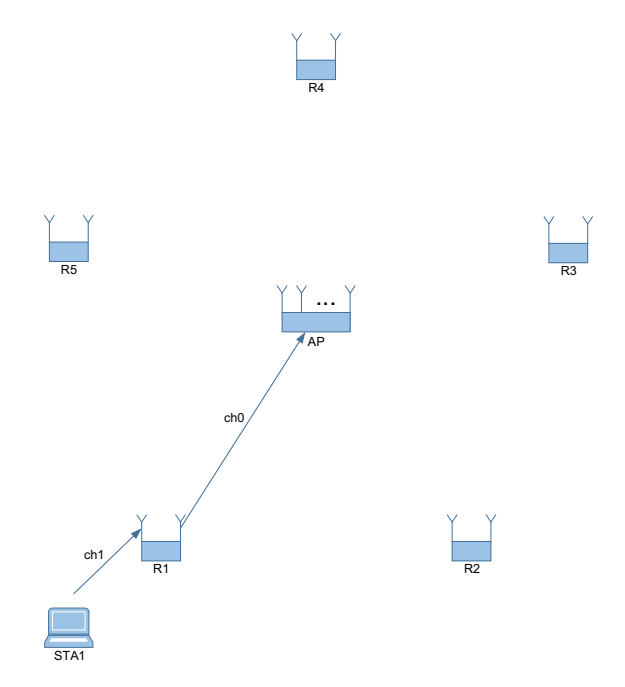


Fig. 3. Relay strategies of AF/DF uplink, deployed with one AP and 5 relays.

 When a relay detects both channels busy or both channels idle, no relaying occurs.

The AP is equipped with multiple MIMO wireless interfaces, which enable it either to receive or transmit on the common channel and all local channels. We also assume that the AP is capable of combining all received copies of a packet from different channels, e.g. with maximum ratio combination (MRC). An MS ready to join the network will choose the relay with strongest signals to associate with, after scanning all local channels.

Let us first consider the downlink in a CAF network. As

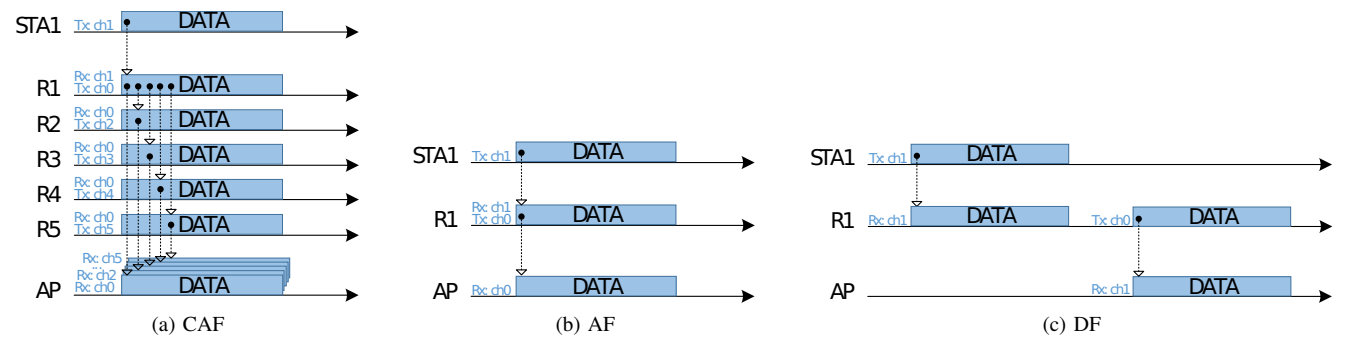


Fig. 4. Data transmissions over the uplink of a relay system, deployed with one AP and five relays using (a) CAF, (b) AF and (c) DF schemes (as in Figs. 1-3), as well as the channels used for transmission (Tx) and reception (Rx).

shown in Fig. 2, when the AP has a downlink packet to send, it transmits the packet on the common channel when all channels are idle. Every relay, on reception of the signal from the common channel, forwards it to its local channel, and thus to the MS(s) listening on the local channel.

The uplink scenario in CAF network is shown in Fig. 1. Uplink packets sent out from an MS (STA1) are received by its local relay (R1) and directly forwarded to the AP through a transmission on the common channel. In addition, the packet, forwarded by the local relay (R1) to the common channel, is received by other relays (R2 - R5), which in turn forward the transmission again from the common channel to their local channels (ch2 - ch5). We refer to this re-forwarding of the transmissions as cooperative amplify and forward (CAF), as the other relays (R2 - R5) are helping forward the transmission from the original relay R1. Finally, duplicated packets forwarded from different relays are combined at the AP.

B. Multi-channel AF and DF Relay Strategy

For convenience, channel settings in multi-channel AF and DF are kept the same as discussed in CAF strategy. The downlink/uplink of AF and DF network are respectively shown in Figs. 2 and 3. Data transmissions over the uplink of CAF, AF and DF networks are shown in Figs. 4(a) to 4(c) respectively. The difference between AF and DF networks is that AF relays forward physically instantaneously, while the DF relays have to wait until the entire packet is received, decode and re-encode the packet, and then contend, the same as a WLAN station, for the media before transmitting.

III. SYSTEM MODEL

Throughout this paper, we use following notations. Bold uppercase letters are matrices, bold lowercase letters are vectors. Symbols $Tr(\cdot)$, $(\cdot)^{\dagger}$, $E[\cdot]$ are trace, hermitian and mean operators, respectively.

A. System Model for CAF Downlink

For modeling the CAF downlink, shown in Fig. 5, we consider wireless links between the following wireless terminals: an AP using K_a antennas for the downlink, a half-duplex AF relay R_i with K_r antennas at the receiver end and K_r antennas at the transmitter end, and a station (STA) equipped with K_s

antennas. We assume no direct link between the AP and the STA. For the wireless link from AP to the relay R_i and the wireless link from R_i to STA, the received signal vectors can be modeled as $\mathbf{r}_{R_i} \in \mathbb{C}^{K_r \times 1}$ and $\mathbf{r}_S \in \mathbb{C}^{K_s \times 1}$ respectively:

$$\mathbf{r}_{R_i} = \mathbf{H}_{AP,R_i} \mathbf{F}_{AP} \mathbf{s} + \mathbf{n}_{R_i}, \tag{1}$$

$$\mathbf{r}_S = \mathbf{H}_{R_i,S} \mathbf{Q}_i \mathbf{r}_{R_i} + \mathbf{n}_S, \tag{2}$$

where $\mathbf{s} \in \mathbb{C}^{K_a \times 1}$ is the signal vector from the AP comprising K_a different symbols, $\mathbf{F}_{AP} \in \mathbb{C}^{K_a \times K_a}$ and $\mathbf{Q}_i \in \mathbb{C}^{K_r \times K_r}$ represent the precoding matrix at the AP and forwarding matrix at the relay \mathbf{R}_i , $\mathbf{H}_{AP,R_i} \in \mathbb{C}^{K_r \times K_a}$ is the channel fading matrix of the first hop link, while $\mathbf{H}_{R_i,S} \in \mathbb{C}^{K_s \times K_r}$ is the channel fading matrix of the second hop link; $\mathbf{n}_{R_i} \in \mathbb{C}^{K_s \times 1}$ and $\mathbf{n}_S \in \mathbb{C}^{K_s \times 1}$ are the additive white Gaussian noises (AWGNs) at relay \mathbf{R}_i and STA respectively, having zero mean and covariance matrices $N_{R_i}\mathbf{I}_{K_r}$ and $N_S\mathbf{I}_{K_r}$, where \mathbf{I}_{K_r} and \mathbf{I}_{K_s} stand for the $K_r \times K_r$ and $K_s \times K_s$ identity matrices. Finally, the estimated signal at the STA is:

$$\hat{\mathbf{r}}_S = \mathbf{G}_{STA}^{\dagger} \mathbf{r}_S, \tag{3}$$

where $\mathbf{G}_{STA} \in \mathbb{C}^{K_s \times K_r}$ is a receive matrix designed optimal for minimizing the mean square error (MSE) $E\left[(\hat{\mathbf{r}}_S - \mathbf{s})(\hat{\mathbf{r}}_S - \mathbf{s})^{\dagger}\right]$, which is also known as the Wiener filter. The optimal receiver matrix \mathbf{G}_{STA} in (3) can be designed as [25] [26]:

$$\mathbf{G}_{STA} = \left(\overline{\mathbf{H}}_{AP,S}\overline{\mathbf{H}}_{AP,S}^{\dagger} + \overline{\mathbf{n}}\right)^{-1}\overline{\mathbf{H}}_{AP,S},\tag{4}$$

where $\overline{\mathbf{H}}_{AP,S} \in \mathbb{C}^{K_s \times K_a}$ is the equivalent channel matrix from AP to STA defined as following:

$$\overline{\mathbf{H}}_{AP,S} = \mathbf{H}_{R_i,S} \mathbf{O}_i \mathbf{H}_{AP,R_i} \mathbf{F}_{AP}, \tag{5}$$

and $\overline{\mathbf{n}}$ is the equivalent noise variance matrix, which can be written as:

$$\overline{\mathbf{n}} = N_{R_i} \mathbf{H}_{R_i, S} \mathbf{Q}_i \mathbf{Q}_i^{\dagger} \mathbf{H}_{R_i, S}^{\dagger} + N_S \mathbf{I}_{R_s}. \tag{6}$$

For the optimal design of transmit matrix \mathbf{F}_{AP} and forwarding matrix \mathbf{Q}_i , we follow the approach widely adopted in the optimal joint transceiver design as in [2], [25], [27], [28],

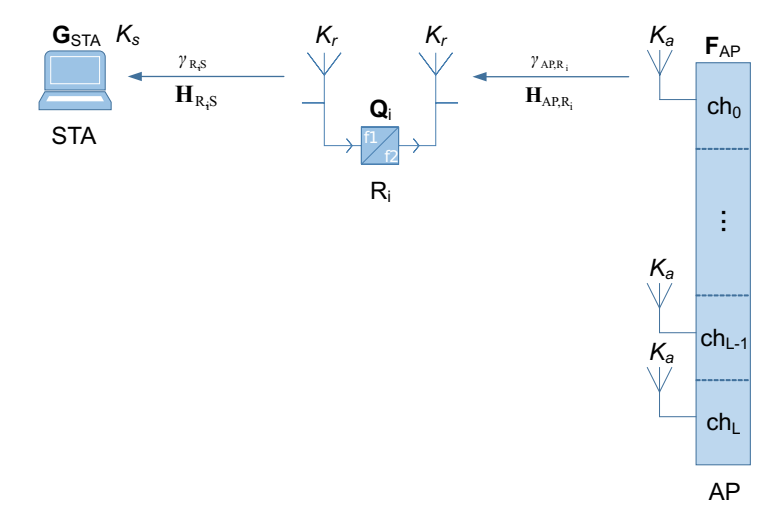


Fig. 5. CAF downlink physical layer model with a mobile station (STA), a relay R_i , and an AP. On each link we show the channel matrix as $\mathbf{H}_{U,V}$ and the instantaneous SNR as $\gamma_{U,V}$.

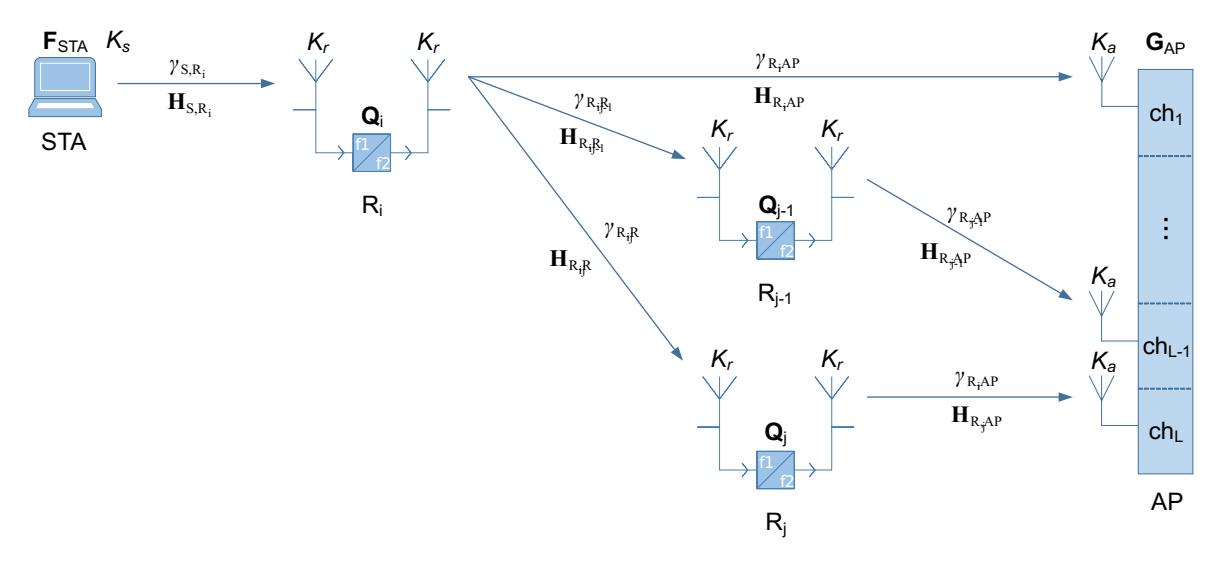


Fig. 6. CAF uplink physical layer model with a station, the first-hop relay R_i , the second-hop relays R_{j-1} , R_j and an access point. On each link we show the channel matrix as $\mathbf{H}_{U,V}$ and the instantaneous SNR as $\gamma_{U,V}$.

by solving the following linear programming optimization problem:

$$\min_{\mathbf{F}_{AP}, \mathbf{Q}_{i}} E\left[(\hat{\mathbf{r}}_{S} - \mathbf{s})(\hat{\mathbf{r}}_{S} - \mathbf{s})^{\dagger} \right]
\text{subject to} Tr(\mathbf{F}_{AP}\mathbf{F}_{AP}^{\dagger}) \leq P_{T},$$

$$Tr(\mathbf{Q}_{i}\mathbf{r}_{R_{i}}\mathbf{r}_{R_{i}}^{\dagger}\mathbf{Q}_{i}^{\dagger}) \leq P_{R},$$
(7)

where P_T and P_R are the power constraints of AP and relays respectively.

B. System Model for CAF Uplink

As shown in Fig. 6, we consider CAF uplinks between the following wireless terminals: a station STA equipped with K_s antennas, L half-duplex AF relays with K_r antennas each at the receiver end and K_r antennas each at the transmitter end, an AP having K_a antennas for each of the L orthogonal channels. We assume no direct link exists between station STA and AP.

For the wireless link from station STA to its first-hop relay R_i , the received vector $\mathbf{r}_{R_i} \in \mathbb{C}^{K_r \times 1}$ at relay R_i is modeled as:

$$\mathbf{r}_{R_i} = \mathbf{H}_{S,R_i} \mathbf{F}_{STA} \mathbf{s} + \mathbf{n}_{R_i}, \tag{8}$$

where $\mathbf{H}_{S,R_i} \in \mathbb{C}^{K_r \times K_s}$ is the first-hop channel fading matrix, $\mathbf{F}_{STA} \in \mathbb{C}^{K_s \times K_s}$ is the precoding matrix at the STA, $\mathbf{s} \in \mathbb{C}^{K_s \times 1}$ is the original signal vector comprising K_s symbols sent from station STA, and $\mathbf{n}_{R_i} \in \mathbb{C}^{K_r \times 1}$ represents the AWGN at \mathbf{R}_i with zero mean and covariance matrix $N_{R_i}\mathbf{I}_{K_r}$, where \mathbf{I}_{K_r} is the $K_r \times K_r$ identity matrix.

Upon reception of the signal \mathbf{r}_{R_i} from STA, the first-hop relay R_i multiplies it with the relay transceiver matrix $\mathbf{Q}_i \in \mathbb{C}^{K_r \times K_r}$ and broadcasts the signal to the AP and second-hop relays R_j . Consequently the signal vectors received at the AP on channel i and relay R_j can be expressed as:

$$\mathbf{r}_{AP_i} = \mathbf{H}_{R_i,AP} \mathbf{Q}_i \mathbf{r}_{R_i} + \mathbf{n}_{AP_i}, \tag{9}$$

$$\mathbf{r}_{R_i} = \mathbf{H}_{R_i, R_i} \mathbf{Q}_i \mathbf{r}_{R_i} + \mathbf{n}_{R_i}, \tag{10}$$

where $\mathbf{H}_{R_i,AP} \in \mathbb{C}^{K_a \times K_r}$ and $\mathbf{H}_{R_i,R_j} \in \mathbb{C}^{K_r \times K_r}$ are the channel fading matrices from R_i to the AP, and from R_i to R_j respectively; the AWGN at AP on channel i is denoted as $\mathbf{n}_{AP_i} \in \mathbb{C}^{K_a \times 1}$, with zero mean and covariance matrix $N_{AP_i}\mathbf{I}_{K_a}$, where \mathbf{I}_{K_a} is the $K_a \times K_a$ identity matrix; the AWGN at R_j is represented by $\mathbf{n}_{R_j} \in \mathbb{C}^{K_r \times 1}$, having zero mean and covariance matrix $N_{R_i}\mathbf{I}_{K_r}$.

Similarly we model the link from the second-hop relay R_j to AP as:

$$\mathbf{r}_{AP_i} = \mathbf{H}_{R_i,AP} \mathbf{Q}_i \mathbf{r}_{R_i} + \mathbf{n}_{AP_i},\tag{11}$$

where $\mathbf{r}_{AP_j} \in \mathbb{C}^{K_a \times 1}$ is the received vector at AP from relay \mathbf{R}_j ; $\mathbf{H}_{R_j,AP} \in \mathbb{C}^{K_a \times K_r}$ is the third-hop channel fading matrix; $\mathbf{n}_{AP_j} \in \mathbb{C}^{K_a \times 1}$ denotes the AWGN at AP with zero mean and covariance matrix $N_{AP_j}\mathbf{I}_{R_a}$, where \mathbf{I}_{R_a} is the $K_a \times K_a$ identity matrix. The signal vector received at destination AP over L different branches is:

$$\mathbf{r} = \mathbf{r}_{AP_i} + \sum_{i \neq i} \mathbf{r}_{AP_j}.$$
 (12)

By multiplying the received signal vector \mathbf{r} with a linear combining matrix, we obtain the estimated signal as:

$$\hat{\mathbf{r}} = \mathbf{G}_{AP}^{\dagger} \mathbf{r},\tag{13}$$

where $\mathbf{G}_{AP} \in \mathbb{C}^{K_a \times K_s}$ is a receive matrix designed optimally for minimizing the MSE $E\left[(\mathbf{\hat{r}} - \mathbf{s})(\mathbf{\hat{r}} - \mathbf{s})^{\dagger}\right]$, which is also known as the Wiener filter:

$$\mathbf{G}_{AP} = \left(\overline{\mathbf{H}}_{S,AP}\overline{\mathbf{H}}_{S,AP}^{\dagger} + \overline{\mathbf{n}}\right)^{-1}\overline{\mathbf{H}}_{S,AP},\tag{14}$$

where $\overline{\mathbf{H}}_{S,AP} \in \mathbb{C}^{K_a \times K_s}$ and $\overline{\mathbf{n}}$ denote the equivalent channel matrix and noise vector over L branches from STA to AP:

$$\overline{\mathbf{H}}_{S,AP} = \mathbf{H}_{R_i,AP} \mathbf{Q}_i \mathbf{H}_{S,R_i} \mathbf{F}_{STA} + \sum_{j \neq i} \mathbf{H}_{R_j,AP} \mathbf{Q}_j \mathbf{H}_{R_i,R_j} \mathbf{Q}_i \mathbf{H}_{S,R_i} \mathbf{F}_{STA},$$

$$\overline{\mathbf{n}} = N_{R_{i}} \mathbf{H}_{R_{i},AP} \mathbf{Q}_{i} \mathbf{Q}_{i}^{\dagger} \mathbf{H}_{R_{i},AP}^{\dagger} + \sum_{j \neq i} N_{AP_{j}} \mathbf{I}_{R_{r}}
+ N_{R_{i}} \sum_{j \neq i} \mathbf{H}_{R_{j},AP} \mathbf{Q}_{j} \mathbf{H}_{R_{i},R_{j}} \mathbf{Q}_{i} \mathbf{Q}_{i}^{\dagger} \mathbf{H}_{R_{i},R_{j}}^{\dagger} \mathbf{Q}_{j}^{\dagger} \mathbf{H}_{R_{j},AP}^{\dagger}
+ \sum_{j \neq i} N_{R_{j}} \mathbf{H}_{R_{j},AP} \mathbf{Q}_{j} \mathbf{Q}_{j}^{\dagger} \mathbf{H}_{R_{j},AP}^{\dagger}.$$
(16)

Similar to the CAF downlink, the optimal design of \mathbf{F}_{STA} , \mathbf{Q}_i and \mathbf{Q}_i are determined by [25] [2]:

$$\min_{\mathbf{F}_{STA}, \mathbf{Q}_{i}, \mathbf{Q}_{j}} E\left[\left(\hat{\mathbf{r}} - \mathbf{s}\right)\left(\hat{\mathbf{r}} - \mathbf{s}\right)^{\dagger}\right]$$
subject to
$$Tr(\mathbf{F}_{STA}\mathbf{F}_{STA}^{\dagger}) \leq P_{T},$$

$$Tr(\mathbf{Q}_{i}\mathbf{r}_{R_{i}}\mathbf{r}_{R_{i}}^{\dagger}\mathbf{Q}_{i}^{\dagger}) \leq P_{R},$$

$$Tr(\mathbf{Q}_{j}\mathbf{r}_{R_{j}}\mathbf{r}_{R_{i}}^{\dagger}\mathbf{Q}_{j}^{\dagger}) \leq P_{R},$$

$$Tr(\mathbf{Q}_{j}\mathbf{r}_{R_{j}}\mathbf{r}_{R_{i}}^{\dagger}\mathbf{Q}_{j}^{\dagger}) \leq P_{R},$$
(17)

where P_T and P_R are power constraints of STA and relays respectively. The method adopted to solve this optimization problem follows [25] and [2]. We derive BERs of this design (CAF uplink and downlink) by proposing an analytical solution for multi-branch multi-hop MIMO networks in Section IV, and further evaluate in comparison with numerical results (obtained by using Monte Carlo simulation) of this design in Section V.

IV. HIGH SNR ANALYSIS FOR BER PERFORMANCE

As shown in [25], the average BER of a link with channel matrix \mathbf{H} can be determined by the eigenvalues of $\mathbf{H}^{\dagger}\mathbf{H}$. In the following subsections, we analyzed single-hop and multihop links, and eventually derived the BER expression for a multi-branch multi-hop MIMO (SDM) link. We then adopted these models to obtain the BER of CAF, AF and DF WLANs for their uplink/downlink respectively.

A. Single-hop Analysis

In this subsection, a single-hop MIMO link between the transmitter U and the receiver V is considered, where U and $V \in \{STA, R_i, R_j, AP\}$. We assume uncorrelated Rayleigh flat-fading channels. The channel matrix between the transmitter U and the receiver V is denoted by $\mathbf{H}_{U,V} \in \mathbb{C}^{K_V \times K_U}$, which is normalized by channel pathloss factor $\alpha_{U,V}$ to obtain:

$$\mathbf{H}_{U,V} = \sqrt{\alpha_{U,V}} \tilde{\mathbf{H}}_{U,V},\tag{18}$$

where columns of $\tilde{\mathbf{H}}_{U,V}$ are independent K_V -variate complex Gaussian distributed vectors with unit covariance and zero mean, and $\alpha_{U,V}$ is modeled using the IEEE 802.11 TGn pathloss model [29], assuming no shadowing and keyhole effect.

Given $\lambda_{k(U,V)}$ and $\lambda'_{k(U,V)}$ as the k-th eigenvalues of matrices $\mathbf{H}_{U,V}^{\dagger}\mathbf{H}_{U,V}$ and $\tilde{\mathbf{H}}_{U,V}^{\dagger}\tilde{\mathbf{H}}_{U,V}$ respectively, we have:

$$\lambda_{k(U,V)} = \alpha_{U,V} \lambda'_{k(U,V)}. \tag{19}$$

The beginning part (when $\lambda_{k(U,V)}$ closes to origin) of the PDF of $\lambda_{k(U,V)}$ can be approximated by a McLaurin series as follows, given the high average SNR assumption:

$$f_{\lambda'_{k(U,V)}}\left(\lambda'_{k(U,V)}\right) = a_k \lambda'_{k(U,V)}^{d_k} + o\left(\lambda'_{k(U,V)}^{d_k}\right),$$
 (20)

where $o(\cdot)$ is the little-o notation, a_k and d_k are given by [3]:

$$d_k = (max\{K_U, K_V\} - k + 1)(min\{K_U, K_V\} - k + 1) - 1, (21)$$

$$a_{k} = \frac{\prod_{i=1}^{\min\{K_{U}, K_{V}\}} \left[\left(\min\{K_{U}, K_{V}\} - i \right)! \right]^{-1}}{\prod_{i=1}^{\min\{K_{U}, K_{V}\}} \left(\min\{K_{U}, K_{V}\} - i \right)!} \left| \mathbf{A}(k) \right| \left| \mathbf{B}(k) \right|,$$
(22)

where $\mathbf{A}(k)$, $\mathbf{B}(k)$ are:

$$[\mathbf{A}(k)]_{i,j} = b \left[i + j + 2 \left(\min\{K_U, K_V\} - k \right) \right]!, \quad i, j \in [1, k),$$
(23)

$$[\mathbf{B}(k)]_{i,j} = \frac{2}{\left[b(i+j)^3 - b(i+j)\right]}, \quad i, j \in [1, \min\{K_U, K_V\} - k),$$
(24)

where $b(x) \triangleq max\{K_U, K_V\} - min\{K_U, K_V\} + x$.

Given the PDF of $\lambda'_{k(U,V)}$ in (20), the PDF of $\lambda_{k(U,V)}$ when $\lambda_{k(U,V)}$ is close to zero is:

$$f_{\lambda_{k(U,V)}}\left(\lambda_{k(U,V)}\right) = a_k \alpha_{(U,V)}^{-(d_k+1)} \lambda_{k(U,V)}^{d_k} + o\left(\lambda_{k(U,V)}^{d_k}\right). \tag{25}$$

B. Multi-hop Analysis

We now consider the two types of multi-hop links shown in Fig. 6: the dual-hop link from STA, through R_i , to AP_i , and the triple-hop link from STA, through R_i and R_j , to AP_j , where AP_j refers to the antenna set of the AP that listens on channel j. Using the high SNR assumption, the error covariance matrices \mathbf{E}_{S,AP_i} (the dual-hop link) and \mathbf{E}_{S,AP_j} (the triple-hop link) using MMSE (Minimum Mean Square Error) transceivers can be written as the sum of error covariance matrices of their corresponding single-hop links respectively [8], [30]:

$$\mathbf{E}_{S,AP_i} = \mathbf{E}_{S,R_i} + \mathbf{E}_{R_i,AP_i}. \tag{26}$$

$$\mathbf{E}_{S,AP_{i}} = \mathbf{E}_{S,R_{i}} + \mathbf{E}_{R_{i},R_{i}} + \mathbf{E}_{R_{i},AP_{i}}.$$
 (27)

Assuming high SNR at every single-hop and applying SVD decomposition on both sides of (26) and (27), we obtain:

$$\lambda_{k(S,AP_i)}^{-1} = \lambda_{k(S,R_i)}^{-1} + \lambda_{k(R_i,AP_i)}^{-1}, \tag{28}$$

$$\lambda_{k(S,AP_i)}^{-1} = \lambda_{k(S,R_i)}^{-1} + \lambda_{k(R_i,R_i)}^{-1} + \lambda_{k(R_i,AP_i)}^{-1}.$$
 (29)

Given the PDF of $\lambda_{k(U,V)}$ for a single-hop link between U and V in (25), it can be shown that the PDF of dual-hop equivalent eigenvalue $\lambda_{k(S,AP_i)}$ and the triple-hop equivalent eigenvalue $\lambda_{k(S,AP_i)}$ when the eigenvalues closed to zeros as:

$$f_{\lambda_{k(S,AP_{i})}}(0^{+}) = f_{\lambda_{k(S,R_{i})}}(0^{+}) + f_{\lambda_{k(R_{i},AP_{i})}}(0^{+}) + o(0^{+}), (30)$$

$$f_{\lambda_{k(S,AP_{j})}}(0^{+})$$

$$= f_{\lambda_{k(S,R_{i})}}(0^{+}) + f_{\lambda_{k(R_{i},R_{j})}}(0^{+}) + f_{\lambda_{k(R_{j},AP_{j})}}(0^{+}) + o(0^{+}).$$
(31)

Conclusions above are inspired by [7] and [8], the former of which proposed PDF of SNR in a multi-hop multi-branch SISO network, while the latter discussed the PDF of SNR in a dual-hop MIMO network. See Appendix A and Appendix B for the complete derivations of (30) and (31).

Given the PDF of $\lambda_{k(U,V)}$ in (25), we have:

$$f_{\lambda_{k(S,AP_{l})}}(\lambda_{k(S,AP_{l})}) = c_{l,k}\lambda_{k(S,AP_{l})}^{d_{k}} + o(0^{+}),$$
 (32)

where

$$c_{l,k} = \begin{cases} a_k \left[\alpha_{(S,R_i)}^{-(d_k+1)} + \alpha_{(R_i,AP_i)}^{-(d_k+1)} \right], & l = i; \\ a_k \left[\alpha_{(S,R_i)}^{-(d_k+1)} + \alpha_{(R_i,R_j)}^{-(d_k+1)} + \alpha_{(R_j,AP_j)}^{-(d_k+1)} \right], & l = j. \end{cases}$$
(33)

C. Multi-hop Multi-branch Analysis

We now consider combining of L branches of those multihop links analyzed in the Subsection IV-B. For a geographically sparse deployment of relays transmitting on L orthogonal channels, as shown in Fig. 1, it is reasonable to assume fadings along the L different uplinks of CAF are uncorrelated. Therefore a diversity gain of L is achieved after combining these L copies of the same symbol received.

To compute the average BER of a multi-branch network, we need first derive the joint PDF of all branches' equivalent

 $\lambda_{k(S,AP_l)}$. With high SNR assumption, the joint PDF can be obtained by (34) (Appendix C shows the detailed derivation):

$$f_{\lambda_{k(S,AP)}}\left(\lambda_{k(S,AP)}\right)$$

$$= \int_{0}^{\infty} \cdots \int_{0}^{\infty} \frac{\partial^{L-1} f_{\lambda_{k(S,AP_{l})}}}{\partial \lambda_{k(S,AP_{l})}^{L-1}} \left(\lambda_{k(S,AP_{l})}\right) d\lambda_{k(S,AP_{1})} \cdots d\lambda_{k(S,AP_{L})}$$

$$\approx \int_{0}^{\infty} \cdots \int_{0}^{\infty} \prod_{l=1}^{L} f_{\lambda_{k(S,AP_{l})}} \left(\lambda_{k(S,AP_{l})}\right) d\lambda_{k(S,AP_{1})} \cdots d\lambda_{k(S,AP_{L})}.$$
(34)

According to [31], the average BER of the link between transmitter U and receiver V can be modeled using (35), where g_A and g_B are constants for a specific modulation scheme M, $Q(\cdot)$ is the Q-function [32], P_T and P_N are the average power of transmitter and noise respectively, $\lambda_{k(U,V)}$ and $f_{\lambda_{k(U,V)}}$ represents the k-th eigenvalue of fading channel matrix with pathloss effects considered, and its corresponding PDF.

$$P(k) = \frac{1}{\log_2 M} \times \int_0^\infty g_A Q\left(\sqrt{\frac{g_B \lambda_{k(U,V)} P_T}{P_N}}\right) f_{\lambda_{k(U,V)}}\left(\lambda_{k(U,V)}\right) d\lambda_{k(U,V)}.$$
(35)

A simplified model for high SNR scenarios was presented in [7], which showed that when the average SNR is high, the average BER P(k) in (35) can be approximated by only considering the integral in (35) over the interval where $\lambda_{k(U,V)}$ is small since for the rest of the domain the function Q is practical zero and the integral is negligible [7]. Equation (35) can be then simplified to (36):

$$P(k) \approx \frac{1}{\log_2 M} \times \int_0^D g_A Q\left(\sqrt{\frac{g_B \lambda_{k(U,V)} P_T}{P_N}}\right) f_{\lambda_{k(U,V)}}\left(\lambda_{k(U,V)}\right) d\lambda_{k(U,V)},$$
(36)

where (0, D) is the integral domain satisfies the Assumption 3 (AS3)) in [7].

This conventional approach based on (35) and its simplified version (36) are intuitive but both involve L+1 fold integrations. Alternatively, we proposed a MGF-based approach simplifying the calculation to one-fold integration of a closed-form solution. We first derive the conditional BER of the combined SNR given SNRs of all branches:

$$\gamma_k = \sum_{l=1}^L \gamma_{k(S,AP_l)},\tag{37}$$

as:

$$P_{(S,AP)}^{'}(k)\mid_{\{\gamma_{k}(S,AP_{l})\}_{l=1}^{L}} = \frac{1}{log_{2}M}g_{A}Q\left(\sqrt{g_{B}\sum_{l=1}^{L}\gamma_{k}(S,AP_{l})}\right). \tag{38}$$

Let us denote the PDF of SNR for *l*-th branch link as $f_{\gamma_{k(S,AP_l)}}(\gamma_{k(S,AP_l)})$, and the corresponding MGF as

 $\mathcal{M}_{\gamma_{k(S,AP_I)}}$. By averaging the product of conditional BER for all branches' PDF of SNR, the average BER for the combined links can be obtained as:

$$P(k) = \frac{1}{\log_2 M} \frac{g_A}{\pi} \int_0^{\pi/2} \prod_{l=1}^L \left[\mathcal{M}_{\gamma_{k(S,AP_l)}} \left(-\frac{g_B}{\sin^2 \theta} \right) \right] d\theta.$$
(39)

See Appendix D for the complete derivation of (39).

Referring to the high SNR approximation in [7], the PDF of eigenvalue $\lambda_{k(S,AP_l)}$ can be approximated in the expression of McLaurin series as (40):

$$f_{\lambda_{k}(S,AP_{l})}\left(\lambda_{k}(S,AP_{l})\right) = \begin{cases} 0, & \lambda_{k}(S,AP_{l}) \in \left(\frac{\left[Q^{-1}(0^{+})\right]^{2}}{g_{B}P_{T}/P_{N}},\infty\right); \\ c_{l,k}\lambda_{l,k}d_{k} + o\left(\lambda_{k}(S,AP_{l})d_{k}\right), & otherwise \end{cases},$$
(40)

where $Q^{-1}(0^+)$ is the inverse Q function closed to the origin from the right side. The corresponding MGF can be obtained as (41):

$$\mathcal{M}_{\lambda_{k}(S,AP_{l})}(t) = \frac{(-1)^{d_{k}} c_{l,k}}{t^{d_{k}+1}} (1+d_{k},-tx),$$

$$\lambda_{k}(S,AP_{l}) \in [0,\frac{\left[Q^{-1}(0^{+})\right]^{2}}{g_{B}P_{T}/P_{N}}],$$
(41)

where (\cdot) is the incomplete gamma function [32]. By substituting (41) into $\mathcal{M}_{\gamma_{k(S,AP_{l})}}(t) = \mathcal{M}_{\lambda_{k(S,AP_{l})}}(tP_{T}/P_{N})$ and (39), we obtain the average BER for the multi-branch multi-hop link from STA to AP:

$$P(k) = \frac{g_A \pi^{-1}}{\log_2 M} \int_0^{\frac{\pi}{2}} \prod_{l=1}^{L} \left[\frac{-c_{l,k} \left(d_k + 1, \frac{g_B P_T}{P_N \sin^2 \theta} x \right)}{\left(\frac{g_B P_T}{P_N \sin^2 \theta} \right)^{d_k + 1}} \right] d\theta.$$
(42)

D. BER Analysis for CAF, AF and DF Networks

Given the BER analysis for a general cooperative network in the Subsection IV-C, we first consider the CAF network. Shown in Fig. 5 and Fig. 6, CAF downlink is a single-branch dual-hop link, while CAF uplink comprises L branches: one dual-hop, and L-1 triple-hop links. By substituting (43) and (33) into (42) respectively, we can obtain the average BERs for CAF downlink and uplink.

$$c_{l,k} = a_k \left[\alpha_{(AP,R_i)}^{-(d_k+1)} + \alpha_{(R_i,S)}^{-(d_k+1)} \right], \tag{43}$$

$$c_{l,k} = \begin{cases} a_k \left[\alpha_{(S,R_i)}^{-(d_k+1)} + \alpha_{(R_i,AP_i)}^{-(d_k+1)} \right], & l = i; \\ a_k \left[\alpha_{(S,R_i)}^{-(d_k+1)} + \alpha_{(R_i,AP_i)}^{-(d_k+1)} + \alpha_{(R_j,AP_j)}^{-(d_k+1)} \right], & l = j. \end{cases} \tag{44}$$

The BER analysis of AF network is similar with CAF network, except the AF network comprises only one single-branch dual-hop for both downlink and uplink.

For the DF network, packets are decoded, re-encoded, and forwarded hop-by-hop. Upon reception of a packet on each hop, receivers check the packet's Cyclic Redundancy Check (CRC) and drop it if there exists an error. Let us denote $P(S,R_i)(k)$ and $P(R_i,AP)(k)$ as the first and second hop BER

for the DF uplink. Similarly, $P_{(AP,R_i)}(k)$ and $P_{(R_i,S)}(k)$ are denoted as the first and second hop BER for the DF downlink. These BERs can be derived by substituting PDFs of $\lambda_{k(U,V)}$ for every single hop link, given in (25), into (35) respectively. Then, the BER of DF network uplink can be modeled as:

$$P(k) = 1 - [1 - P_{(S,R_i)}(k)] [1 - P_{(R_i,AP)}(k)].$$
 (45)

Similarly, the BER for the downlink of the DF network can be modeled as:

$$P(k) = 1 - [1 - P_{(AP,R_i)}(k)] [1 - P_{(R_i,S)}(k)].$$
 (46)

E. Coding Gain

While uncoded BER models of CAF, AF and DF networks are derived in Subsection IV-D, for wireless systems in practice (e.g., IEEE 802.11), it is necessary to model the impact of channel coding. According to IEEE 802.11 standards [33] [34], two coding approaches are adopted for forward error correction (FEC) to increase error resilience. The mandatory approach is binary convolutional coding (BCC), while the optional one is low-density parity-check (LDPC). In the context of this paper, we assume BCC is used.

To estimate impact of IEEE 802.11 coding gain to CAF, AF, and DF relay networks, we make following two approximations. First, slow fading is assumed. Second, asymptotic coding gain is used for the estimation. These two approximations give us the upper bound of actual coding gain. According to [35], the asymptotic coding gain $G_c[dB]$ of the BCC encoder/decoder can be modeled as:

$$G_c = 10 \log_{10}(d_{min}R),$$
 (47)

where d_{min} is the minimum Hamming distance between any two different code words, and R is the coding rate. These values are defined in IEEE standards [33] [34]. The coding gain G_c is measured as a reduction of SNR at the receiver necessary to achieve the same BER as a transmission without G_c .

F. Determination of WLAN Coverages

Pathloss models for IEEE 802.11 networks were proposed in an IEEE document [29]. Omitting log-normal shadowing (also known as shadow fading), the pathloss of an IEEE 802.11 link between the transmitter U and receiver V is modeled as:

$$\alpha_{U,V} = PL_{FS}(d_{BP}) + 3.5 \times 10 \log_{10}(d/d_{BP}),$$
 (48)

where d is the distance of the link in meter, d_{BP} is defined as break-point distance with specific values defined in [29], and $PL_{FS}(\cdot)$ is the free space pathloss:

$$PL_{FS}(d_{BP}) = -10\log_{10}\left[G_tG_r\left(\frac{c}{4\pi f d_{BP}}\right)^2\right],$$
 (49)

where G_t and G_r are transmitter and receiver antenna gains in ratios, c is the speed of light in meters per second, and f is the radio frequency in Hz. By substituting (48) into (43) and (44) respectively, we can obtain a BER model that incorporates IEEE 802.11 pathloss for a WLAN using CAF

TABLE II CONFIGURATION PARAMETERS

Parameters	Value	
Number of Antennas Ka	2	
Number of Antennas K_r	2	
Number of Antennas K_s	2	
AP Antenna Gain	2 dBi	
Relay Antenna Gain	2 dBi	
STA Antenna Gain	2 dBi	
AP TX Power	20 dBm	
Relay TX Power	20 dBm	
MS TX Power	15 dBm	
Channel Frequency	5.25 GHz	
Frame Length	1000 Bytes	

scheme. Similarly, we model the BER for a WLAN using AF and DF schemes respectively.

The IEEE 802.11 standards require that, for a particular transmission rate, the Frame Error Rate (FER) of a PSDU with 400 octets should be lower than a threshold of 3% [33]. This is equivalent to a BER threshold $P_{threshold} = 9.5 \times 10^{-6}$. The BER ω_{BER} converts to FER ω_{FER} by:

$$\omega_{FER} = 1 - (1 - \omega_{BER})^{FL},\tag{50}$$

where FL is the frame length in bits. Given a specific modulation scheme, we define the coverage of a relay network as the areas where the BER P(k) is lower than $P_{threshold}$. Specifically, the coverage boundary is obtained by increasing distance d beginning from zero until $P(k) \ge P_{threshold}$.

V. PERFORMANCE EVALUATION

This section evaluates the PHY performance of CAF in comparison to conventional AF and DF networks. We configure all networks with one access point and six auxiliary relays placed symmetrically around the AP. A deployment of more relays would further favor CAF comparing with the other two approaches (AF and DF).

For this simulation, IEEE 802.11 standard parameters and common configuration options are considered. In this paper, we follow IEEE 802.11n-2012, although the results can easily be extended to other variants. Parameters configured in this simulation are shown in the Table II. We assume MIMO SDM for all devices.

Fig. 7 shows the data rates as a function of distance between a STA and the AP, comparing CAF, AF and DF networks. For simplicity, we assume following four modulation schemes (MCSs) are adopted: 64-QAM (2/3), 16-QAM (1/2), QPSK (1/2), and BPSK (1/2)². As described in the Section IV, the CAF downlink is as same as the AF downlink and are therefore shown together. As shown in Fig. 7, CAF significantly outperforms AF and DF in terms of data rates on the uplink while being close to DF on the downlink. Since in practice a usable link requires both an uplink and a downlink, CAF significantly outperforms AF and DF for duplex links.

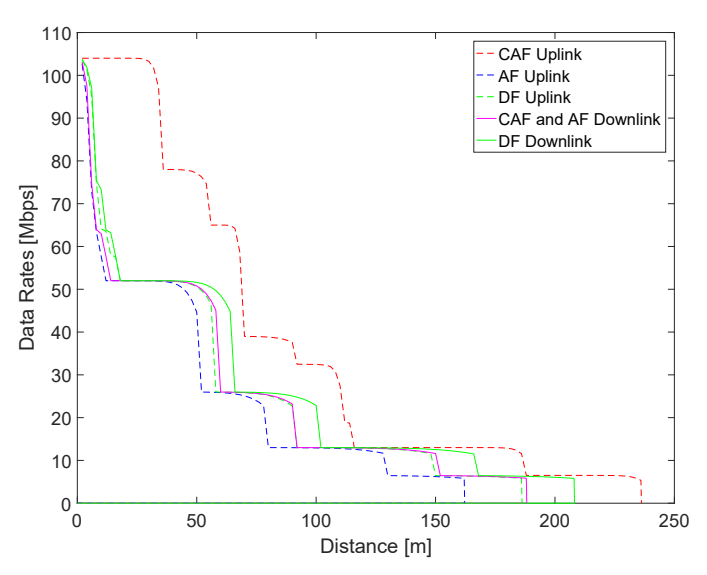


Fig. 7. Date rates for a system employing six relays and using CAF, AF and DF for uplink and downlink as a function of distance between the client and the AP. Noise floor is -55 dBm.

Fig. 8 depicts the uplink uncoded BERs versus equivalent SNR of the same dual-hop link for CAF, AF and DF scenarios, using both theoretical and Monte Carlo simulation results. As illustrated, the uncoded BER of CAF decreases significantly faster than AF and DF approaches while SNR increases. The performance of CAF is due to the larger diversity gain, which is achieved by utilizing all six branches for communication. These branches are considered uncorrelated, given the geographically separated placement and frequency orthogonality of local channels of relays. They reduce the probability that, when a symbol is passed through the system, all branches are severely faded and lead to a symbol estimation error at the AP. Equivalently, that means these redundant branches reduces the ratio of a symbol error (SER). In addition, with MRC at the AP, SNR of a symbol is improved by properly combining six replicas from these branches, which further lowers the SER for CAF.

Figs. 9(a) and 9(b) show two-dimensional uplink and downlink coverage maps of CAF, AF, DF and No-Relay-Forwarding (NF) scenarios with BPSK (1/2) MCS and six auxiliary relays, in terms of the two streams (named the better and worse stream). As shown in Fig. 9(b) downlink coverage of DF network is slightly better than AF network (AF and CAF networks are identical for the downlink), which has been previously reported in [18], [36] for small SNRs. For the uplink coverage, the CAF network outperforms significantly AF and DF networks, for both the better and the worse streams, as signals of CAF uplink benefit from five additional diversity paths. Similar comparison results can also be observed for CAF, AF and DF networks using other MCSs or different channel frequency.

As shown in Figs. 9(a) and 9(b), the worse streams are limited to a shorter range in comparison with the corresponding better streams, since the worse streams have lower diversity gain than the better streams. This performance gap was previously reported in an experimental research [37] for IEEE 802.11n.

 $^{^{2}(2/3)}$ and (1/2) indicate for the FEC rates used.

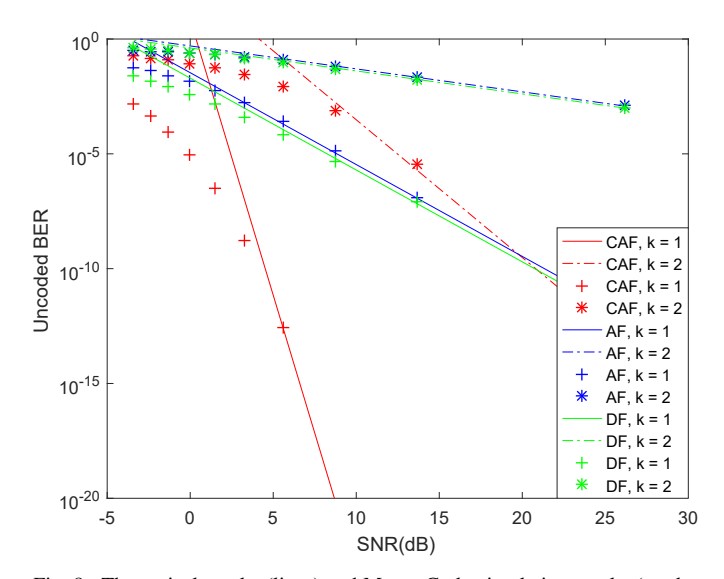


Fig. 8. Theoretical results (lines) and Monte Carlo simulation results (marker dots) for average uncoded BER of k-th stream for a system employing six relays and using CAF, AF and DF for uplink as a function of equivalent SNR of the same dual-hop link STA \rightarrow relay $R_i \rightarrow$ AP.

VI. CONCLUSION AND FUTURE WORK

In this paper, we have proposed a novel cooperative multichannel MIMO relay system to extend the coverage of 802.11 networks with no changes on the IEEE 802.11 standards. It has been shown that CAF network performs significantly better than both conventional AF networks and DF networks.

In the future, we will continue our research on following issues:

- CAF networks with cooperative downlinks.
- CAF networks with MIMO used for beamforming.
- MAC layer performance modeling for CAF, AF and DF networks.

APPENDIX A

Given two random variable X, Y and their PDFs at zero, namely $f_X(0)$ and $f_Y(0)$, the PDF of random variable W = XY/(X+Y) at zero is given as $f_W(0) = f_X(0) + f_Y(0)$.

Proof: Set auxiliary random variable Z = X + Y such that:

$$X = h_1(W, Z) = Z - \frac{Z \pm \sqrt{Z^2 - 4WZ}}{2},$$
 (51)

$$Y = h_2(W, Z) = \frac{Z \pm \sqrt{Z^2 - 4WZ}}{2}.$$
 (52)

Then the Jacobian is:

$$\mathcal{J} = \begin{vmatrix} \frac{\partial h_1(W,Z)}{\partial W} & \frac{\partial h_1(W,Z)}{\partial Z} \\ \frac{\partial h_2(W,Z)}{\partial W} & \frac{\partial h_2(W,Z)}{\partial Z} \end{vmatrix}.$$
 (53)

Substituting W = 0 into (53), we obtain:

$$|\mathcal{J}||_{W=0} = 1. \tag{54}$$

Therefore, we have:

$$f_{WZ}(W, Z) = |\mathcal{J}| f_{XY}(X, Y)$$

= $|\mathcal{J}| f_X(h_1(W, Z)) f_Y(h_2(W, Z))$. (55)

Integrating both sides of (55) over Z:

$$f_W(W) = \int_0^\infty |\mathcal{J}| f_X(h_1(W, Z)) f_Y(h_2(W, Z)) dZ.$$
 (56)

Substituting W = 0, we have:

$$f_{W}(0) = \left[f_{X}(0) \int_{0}^{\infty} |\mathcal{J}| f_{Y} (h_{2}(W, Z)) dY + f_{Y}(0) \int_{0}^{\infty} |\mathcal{J}| f_{X} (h_{1}(W, Z)) dX \right]$$

$$= f_{X}(0) + f_{Y}(0).$$
(57)

APPENDIX B

Given three random variables X, Y, and Z and their PDFs at zeros, namely $f_X(0)$ $f_Y(0)$ and $f_Z(0)$, the PDF of random variable W = XYZ/(XY + YZ + XZ) at zero is given as $f_W(0) = f_X(0) + f_Y(0) + f_Z(0)$.

Proof of this can follow the same method used in Appendix (A). Through setting auxiliary random variable V = X + Z and S = Y - Z, we have $|\mathcal{J}| = \frac{\partial(X,Y,Z)}{\partial(W,V,S)} = 1$ and $f_W(0) = f_X(0) + f_Y(0) + f_Z(0)$. We omit details of calculation.

Alternatively, we can prove this by following approach: *Proof*:

$$Pr(W \le 0^{+}) = 2Pr(X \le 0^{+}) Pr(Y \le 0^{+}) Pr(Z \le 0^{+}) + Pr(X \le 0^{+}) + Pr(Y \le 0^{+}) + Pr(Z \le 0^{+}) - Pr(X \le 0^{+}) Pr(Y \le 0^{+}) - Pr(Y \le 0^{+}) Pr(Z \le 0^{+}) - Pr(X \le 0^{+}) Pr(Z \le 0^{+}).$$
(58)

Writing (58) for their CDFs, we obtain:

$$F_W(0) = F_X(0) + F_Y(0) + F_Z(0) + 2F_X(0)F_Y(0)F_Z(0) - F_X(0)F_Y(0) - F_Y(0)F_Z(0) - F_X(0)F_Z(0).$$
(59)

Given (59) and PDF functions in the form $f_{(\cdot)}(\cdot) = a(\cdot)^d + o((\cdot)^d)$, when $w \to 0^+$, we have

$$f_{W}(w) = f_{X}(w) + f_{Y}(w) + f_{Z}(w) + o\left(w^{min\{d_{X}, d_{Y}, d_{Z}\}}\right).$$
 (60)

A similar approach is found in [8].

APPENDIX C

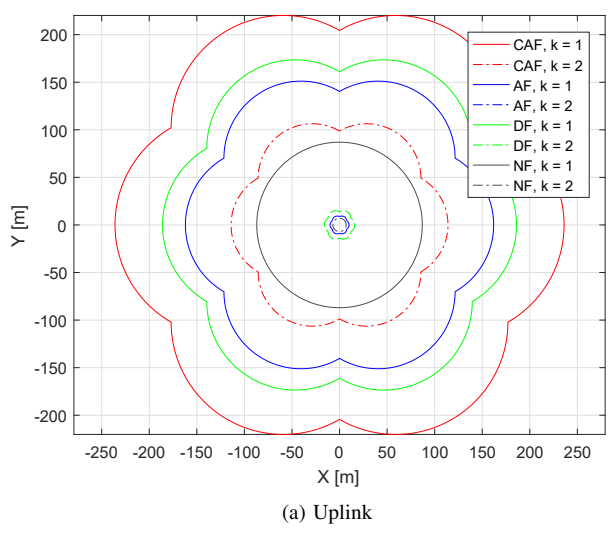
PDF OF SUM OF RANDOM VARIABLES

For N i.i.d random variables X_i with $i \in (1, N)$, we define their sum as Y:

$$Y = \sum_{i=1}^{N} X_i. \tag{61}$$

The Laplace transform of (61) is given by (62) and (63):

$$\mathcal{L}_Y(s) = \prod_{i=1}^N \mathcal{L}_{X_i}(s), \tag{62}$$



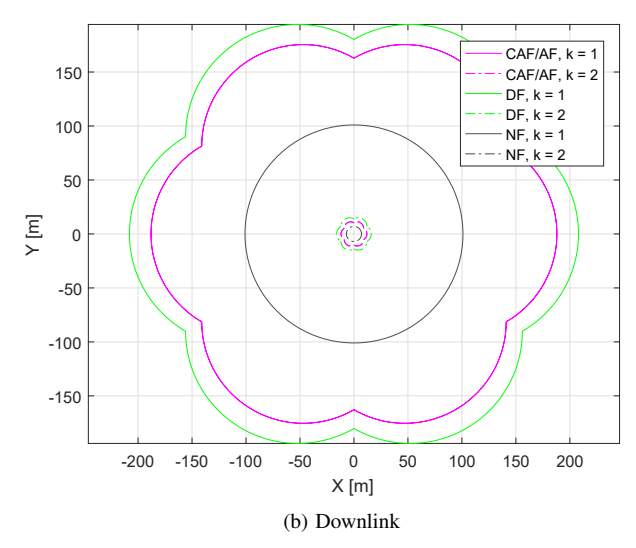


Fig. 9. Uplink and downlink coverage for a 5.25 GHz 2×2 MIMO SDM system with BPSK(1/2) MCS, employing six relays and using CAF, AF, DF and No-Forward (NF) schemes.

$$\int_0^\infty e^{-st} f_Y(t) dt = \prod_{i=1}^N \int_0^\infty e^{-st} f_{X_i}(t) dt.$$
 (63)

From the Initial Value Theorem (IVT), we have:

$$\lim_{t \to 0} f(t) = \lim_{s \to 0} sF(s). \tag{64}$$

Multiplying s to both sides of (63) and take their limits at $s \to \infty$:

$$\lim_{s \to \infty} s \int_0^\infty e^{-st} f_Y(t) dt = \lim_{s \to \infty} s \prod_{i=1}^N \int_0^\infty e^{-st} f_{X_i}(t) dt$$
 (65)

From IVT and (65), we obtain:

$$\lim_{t \to 0} f_Y(t) = \lim_{t \to 0} f_{X_1}(t) \lim_{s \to \infty} \prod_{i=2}^{N} \int_0^\infty e^{-st} f_{X_i}(t) dt.$$
 (66)

Again, multiplying s to both sides and take their limits at $s \to \infty$:

$$\lim_{s \to \infty} s \left[\lim_{t \to 0} f_Y(t) \right] = \lim_{s \to \infty} s \left[\lim_{t \to 0} f_{X_i}(t) \lim_{s \to \infty} \prod_{i=2}^{N} \int_0^\infty e^{-st} f_{X_i}(t) dt \right]. \tag{67}$$

Then, we obtain:

$$\lim_{t \to 0} \frac{\partial f_Y}{\partial Y}(t) = \lim_{t \to 0} f_{X_1}(t) \lim_{t \to 0} f_{X_2}(t) \left[\lim_{s \to \infty} \prod_{i=3}^{N} \int_0^\infty e^{-st} f_{X_i}(t) dt \right]. \tag{68}$$

Multiply s^{N-2} to both sides of (68) and repeat IVT for N-2 times, we finally obtain:

$$\lim_{t \to 0} \frac{\partial^{N-1} f_Y}{\partial Y^{N-1}}(t) = \prod_{i=1}^{N} \lim_{t \to 0} f_{X_i}(t).$$
 (69)

Consequently, we obtained

$$\frac{\partial^{N-1} f_Y}{\partial Y^{N-1}}(0) = \prod_{i=1}^{N} f_{X_i}(0).$$
 (70)

APPENDIX D DERIVATION OF EQUATION (39)

ts at
$$\begin{aligned}
&P(k) = \int_{0}^{\infty} \cdots \int_{0}^{\infty} \left[\frac{1}{\log_{2} M} g_{A} Q \left(\sqrt{g_{B}} \sum_{l=1}^{L} \gamma_{k(S,AP_{l})} \right) \right] \\
&\times \prod_{l=1}^{L} f_{\gamma_{k(S,AP_{l})}} \left(\gamma_{k(S,AP_{l})} \right) d\gamma_{k(S,AP_{l})} \cdots d\gamma_{k(S,AP_{L})} \\
&= \int_{0}^{\infty} \cdots \int_{0}^{\infty} \left[\frac{1}{\log_{2} M} \frac{g_{A}}{\pi} \int_{0}^{\pi/2} \prod_{l=1}^{L} exp \left(-\frac{g_{B} \gamma_{k(S,AP_{l})}}{\sin^{2} \theta} \right) \right] \\
&\times f_{\gamma_{k(S,AP_{l})}} \left(\gamma_{k(S,AP_{l})} \right) d\theta d\gamma_{k(S,AP_{l})} \cdots d\gamma_{k(S,AP_{L})} \\
&= \frac{1}{\log_{2} M} \frac{g_{A}}{\pi} \prod_{l=1}^{L} \left[\int_{0}^{\infty} \int_{0}^{\pi/2} exp \left(-\frac{g_{B} \gamma_{k(S,AP_{l})}}{\sin^{2} \theta} \right) \right] \\
&\times f_{\gamma_{k(S,AP_{l})}} \left(\gamma_{k(S,AP_{l})} \right) d\theta d\gamma_{k(S,AP_{l})} \\
&= \frac{1}{\log_{2} M} \frac{g_{A}}{\pi} \int_{0}^{\pi/2} \prod_{l=1}^{L} \left[M_{\gamma_{k(S,AP_{l})}} \left(-\frac{g_{B}}{\sin^{2} \theta} \right) \right] d\theta.
\end{aligned} \tag{71}$$

REFERENCES

- S. R. Group, 2016. [Online]. Available: https://www.aptilo.com/mobileoperators-carrier-wifi-offload-hetnet
- [2] D. P. Palomar, J. M. Cioffi, and M. A. Lagunas, "Joint tx-rx beamforming design for multicarrier mimo channels: A unified framework for convex optimization," *IEEE Transactions on Signal Processing*, vol. 51, no. 9, pp. 2381–2401, 2003.
- [3] L. G. Ordóñez, D. P. Palomar, A. Pagès-Zamora, and J. Fonollosa, "High-SNR analytical performance of spatial multiplexing MIMO systems with CSI," *IEEE Transactions on Signal Processing*, vol. 55, no. 11, pp. 5447–5463, 2007.
- [4] M. Simon and M. Alouini, *Digital Communication over Fading Chan-nels*, ser. Wiley Series in Telecommunications and Signal Processing. Wiley, 2000.

- [5] —, Digital Communication over Fading Channels, ser. Wiley Series in Telecommunications and Signal Processing. Wiley, 2005.
- [6] M. Kang and M.-S. Alouini, "A comparative study on the performance of MIMO MRC systems with and without co-channel interference," in *Communications*, 2003. ICC'03. IEEE International Conference on, vol. 3. IEEE, 2003, pp. 2154–2158.
- [7] Z. Wang and G. B. Giannakis, "A simple and general parameterization quantifying performance in fading channels," *IEEE Transactions on Communications*, vol. 51, no. 8, pp. 1389–1398, 2003.
- [8] C. Song, K.-J. Lee, and I. Lee, "Performance analysis of mmse-based amplify and forward spatial multiplexing MIMO relaying systems," *IEEE Transactions on Communications*, vol. 59, no. 12, pp. 3452–3462, 2011.
- [9] —, "Mmse-based mimo cooperative relaying systems: Closed-form designs and outage behavior," *IEEE Journal on Selected Areas in Communications*, vol. 30, no. 8, pp. 1390–1401, 2012.
- [10] G. Amarasuriya, C. Tellambura, and M. Ardakani, "Performance analysis of hop-by-hop beamforming for dual-hop MIMO AF relay networks," Communications, IEEE Transactions on, vol. 60, no. 7, pp. 1823–1837, 2012
- [11] M. O. Hasna and M.-S. Alouini, "Harmonic mean and end-to-end performance of transmission systems with relays," *Communications*, *IEEE Transactions on*, vol. 52, no. 1, pp. 130–135, 2004.
- [12] M. Arti and M. R. Bhatnagar, "Maximal ratio transmission in AF MIMO relay systems over nakagami-fading channels," *IEEE Transactions on Vehicular Technology*, vol. 64, no. 5, pp. 1895–1903, 2015.
- [13] A. Ribeiro, X. Cai, and G. B. Giannakis, "Symbol error probabilities for general cooperative links," *IEEE Transactions on wireless commu*nications, vol. 4, no. 3, pp. 1264–1273, 2005.
- [14] D. Darsena, G. Gelli, F. Melito, and F. Verde, "Performance analysis of amplify-and-forward multiple-relay mimo systems with zf reception," *IEEE Transactions on Vehicular Technology*, vol. 64, no. 7, pp. 3274– 3280, 2015.
- [15] M. Vehkapera, L. Rasmussen, and M. Girnyk, "Asymptotic performance analysis of a k-hop amplify-and-forward relay MIMO channel," *IEEE Transactions on Information Theory*, 2016.
- [16] S. Barghi and H. Jafarkhani, "Exploiting asynchronous amplify-and-forward relays to enhance the performance of IEEE 802.11 networks," IEEE/ACM Transactions on Networking (TON), vol. 23, no. 2, pp. 479–490, 2015.
- [17] A. H. Forghani, S. Aïssa, and M. Xia, "Analysis of reactive multibranch relaying under interference and nakagami-m fading," in Wireless Communications and Mobile Computing Conference (IWCMC), 2017 13th International. IEEE, 2017, pp. 1945–1950.
- [18] V. Asghari, A. Maaref, and S. Aissa, "Symbol error probability analysis for multihop relaying over nakagami fading channels," in *Wireless Communications and Networking Conference (WCNC)*, 2010 IEEE. IEEE, 2010, pp. 1–6.
- [19] M. R. Bhatnagar, "Performance analysis of a path selection scheme in multi-hop decode-and-forward protocol," *IEEE Communications Letters*, vol. 16, no. 12, pp. 1980–1983, 2012.
- [20] M. R. Bhatnagar, R. K. Mallik, and O. Tirkkonen, "Performance evaluation of best-path selection in a multihop decode-and-forward cooperative system," *IEEE Transactions on Vehicular Technology*, vol. 65, no. 4, pp. 2722–2728, 2016.
- [21] M. R. Bhatnagar and M. Arti, "Selection beamforming and combining in decode-and-forward MIMO relay networks," *IEEE Communications Letters*, vol. 17, no. 8, pp. 1556–1559, 2013.
- [22] M. Arti, R. K. Mallik, and R. Schober, "Performance analysis of ostbc relaying in AF MIMO relay systems with imperfect CSI," *IEEE Transactions on Vehicular Technology*, vol. 64, no. 7, pp. 3291–3298, 2015
- [23] M. Kang and M.-S. Alouini, "Largest eigenvalue of complex Wishart matrices and performance analysis of MIMO MRC systems," *Selected Areas in Communications, IEEE Journal on*, vol. 21, no. 3, pp. 418–426, 2003.
- [24] N. Okati, B. Razeghi, and M. R. Mosavi, "On relay selection to maximize coverage region for cooperative cellular networks with multiple fixed and unfixed relays," in 2015 6th International Conference on Computing, Communication and Networking Technologies (ICCCNT). IEEE, 2015, pp. 1–6.
- [25] L. Sanguinetti, A. A. D'Amico, and Y. Rong, "A tutorial on the optimization of amplify-and-forward MIMO relay systems," *IEEE Journal on Selected Areas in Communications*, vol. 30, no. 8, pp. 1331–1346, 2012.
- [26] E. Perahia and R. Stacey, Next generation wireless LANs: 802.11 n and 802.11 ac. Cambridge university press, 2013.

- [27] Y. Rong and Y. Hua, "Optimality of diagonalization of multi-hop MIMO relays," *IEEE Transactions on Wireless Communications*, vol. 8, no. 12, 2009.
- [28] A. Toding, M. Khandaker, and Y. Rong, "Optimal joint source and relay beamforming for parallel MIMO relay networks," in *Proceedings of the* 6th International Conference on Wireless Communications, Networking and Mobile Computing. IEEE, 2010.
- [29] V. Erceg and et al., "Tgn channel models," *IEEEdoc* 802.11-03/940r3, 2004.
- [30] C. Song, K.-J. Lee, and I. Lee, "Mmse based transceiver designs in closed-loop non-regenerative mimo relaying systems," *IEEE Transac*tions on Wireless Communications, vol. 9, no. 7, pp. 2310–2319, 2010.
- [31] K. Cho and D. Yoon, "On the general BER expression of one-and twodimensional amplitude modulations," *IEEE Transactions on Communi*cations, vol. 50, no. 7, pp. 1074–1080, 2002.
- [32] D. Zwillinger, Table of integrals, series, and products. Elsevier, 2014.
- [33] IEEE Std. 802.11-2012: Wireless Medium Access Control (MAC) and Physical Layer (PHY) specifications. [Online]. Available: http://standards.ieee.org/getieee802/download/802.11-2012.pdf
- [34] IEEE Std. 802.11ac-2013: Wireless Medium Access Control (MAC) and Physical Layer (PHY) specifications - Amendment 4. [Online]. Available: http://standards.ieee.org/getieee802/download/802.11ac-2013.pdf
- [35] R. Johannesson and K. S. Zigangirov, Fundamentals of convolutional coding. John Wiley & Sons, 2015, vol. 15.
- [36] C. Hucher, G. R.-B. Othman, and J.-C. Belfiore, "Af and df protocols based on alamouti st code," in 2007 IEEE International Symposium on Information Theory. IEEE, 2007, pp. 1526–1530.
- [37] K. Pelechrinis, T. Salonidis, H. Lundgren, and N. Vaidya, "Experimental characterization of 802.11 n link quality at high rates," in *Proceedings* of the fifth ACM international workshop on Wireless network testbeds, experimental evaluation and characterization. ACM, 2010, pp. 39–46.



Yuepeng Qi is currently a Ph.D. candidate with the Department of Computer Science, North Carolina State University, Raleigh, NC, USA. He received the B.E. degree in software engineering from Xi'an Jiaotong University, Xi'an, China, and the M.S. degree in IT Convergence Engineering from Pohang University of Science and Technology, Pohang, Republic of Korea, in 2011 and 2014, respectively. His research interests include PHY and MAC layers of wireless networks, and IEEE 802.11 networks in particular.



modeling and support.

Mihail L. Sichitiu received the Ph.D. degree in electrical engineering from the University of Notre Dame, Notre Dame, IN, USA, in 2001. He is currently a Professor with the Department of Electrical and Computer Engineering, North Carolina State University, Raleigh, NC, USA. He is teaching wireless networking and UAV courses. His research interests include networking in general and multihop wireless networks in particular. In these systems, he is studying problems related to localization, time synchronization, routing, fairness, and mobility